Acta Pharmacologica Sinica

www.nature.com/aps

ARTICLE

TGR5 agonist inhibits intestinal epithelial cell apoptosis via cAMP/PKA/c-FLIP/JNK signaling pathway and ameliorates dextran sulfate sodium-induced ulcerative colitis

Wen-ji Yang[1,2], Fang-hui Han[1], Yi-pei Gu[1], Hui Qu[1], Jia Liu[3], Jian-hua Shen[1,2]✉ and Ying Leng[1,2]✉

Excessive apoptosis of intestinal epithelial cell (IEC) is a crucial cause of disrupted epithelium homeostasis, leading to the pathogenesis of ulcerative colitis (UC). The regulation of Takeda G protein-coupled receptor-5 (TGR5) in IEC apoptosis and the underlying molecular mechanisms remained unclear, and the direct evidence from selective TGR5 agonists for the treatment of UC is also lacking. Here, we synthesized a potent and selective TGR5 agonist OM8 with high distribution in intestinal tract and investigated its effect on IEC apoptosis and UC treatment. We showed that OM8 potently activated hTGR5 and mTGR5 with EC_{50} values of 202 ± 55 nM and 74 ± 17 nM, respectively. After oral administration, a large amount of OM8 was maintained in intestinal tract with very low absorption into the blood. In DSS-induced colitis mice, oral administration of OM8 alleviated colitis symptoms, pathological changes and impaired tight junction proteins expression. In addition to enhancing intestinal stem cell (ISC) proliferation and differentiation, OM8 administration significantly reduced the rate of apoptotic cells in colonic epithelium in colitis mice. The direct inhibition by OM8 on IEC apoptosis was further demonstrated in HT-29 and Caco-2 cells in vitro. In HT-29 cells, we demonstrated that silencing TGR5, inhibition of adenylate cyclase or protein kinase A (PKA) all blocked the suppression of JNK phosphorylation induced by OM8, thus abolished its antagonizing effect against TNF-α induced apoptosis, suggesting that the inhibition by OM8 on IEC apoptosis was mediated via activation of TGR5 and cAMP/PKA signaling pathway. Further studies showed that OM8 upregulated cellular FLICE-inhibitory protein (c-FLIP) expression in a TGR5-dependent manner in HT-29 cells. Knockdown of c-FLIP blocked the inhibition by OM8 on TNF-α induced JNK phosphorylation and apoptosis, suggesting that c-FLIP was indispensable for the suppression of OM8 on IEC apoptosis induced by OM8. In conclusion, our study demonstrated a new mechanism of TGR5 agonist on inhibiting IEC apoptosis via cAMP/PKA/c-FLIP/JNK signaling pathway in vitro, and highlighted the value of TGR5 agonist as a novel therapeutic strategy for the treatment of UC.

Keywords: TGR5 agonist; ulcerative colitis; intestinal epithelial cell; apoptosis; cAMP/PKA signaling pathway; c-FLIP

Acta Pharmacologica Sinica (2023) 44:1649–1664; https://doi.org/10.1038/s41401-023-01081-y

INTRODUCTION

Ulcerative colitis (UC) is a kind of inflammatory bowel disease (IBD) that affects the colon involving the mucosal and submucosal layers [1, 2]. Although the precise etiology of UC is still relatively unknown, the breakdown of intestinal epithelial barrier has been demonstrated to play a key role in the process of UC [3, 4]. Destruction of intestinal epithelial homeostasis, manifested by increased intestinal epithelial cell (IEC) apoptosis in activated intestinal inflammatory regions of UC patients and murine colitis, is tightly associated with defects in intestinal epithelial barrier [5, 6]. IEC apoptosis occurs in the early stage of UC, and excessive IEC apoptosis disrupts the epithelial defense system, facilitating the invasion of luminal antigens, triggering an inflammatory cascade and driving disease progression [7, 8]. Aberrant activation of apoptotic pathways in response to inflammatory stimuli such as tumor necrosis factor-alpha (TNF-α) are involved in the UC pathology [9–11]. Thus, identifying agents that protect colonic epithelial cells from apoptosis and restore the integrity of the gut barrier might be helpful for the control of disease flares and provide an invaluable strategy to the treatment of UC.

Takeda G protein-coupled receptor-5 (TGR5, also known as GP-BAR1) belongs to the family of G-protein coupled receptors (GPCRs) and is ubiquitously expressed in various tissues, such as gallbladder, brown adipose and intestinal tract [12]. Activation of TGR5 in enteroendocrine L cells of intestinal tract promotes the secretion of incretins including glucagon-like peptide-1 (GLP-1) and glucagon-like peptide-2 (GLP-2) [13]. TGR5 agonist has shown promise in treating metabolic disease by elevating GLP-1 levels [14]. Recently, a few studies provided interesting clues that TGR5 activation modulates intestinal epithelial barrier integrity. $TGR5^{-/-}$ mice exhibited impaired colonic mucosal epithelial morphology, abnormal tight junction structure, increased intestinal permeability and were more susceptible to DSS-induced colitis [15]. Deletion of TGR5 in the intestinal stem cell of mice resulted in reduction of the proliferation and regeneration of crypt compartment and accelerated the onset and progression of DSS-induced

[1]State Key Laboratory of Drug Research, Shanghai Institute of Materia Medica, Chinese Academy of Sciences, Shanghai 201203, China; [2]University of Chinese Academy of Sciences, Beijing 100049, China and [3]Shanghai Institute of Materia Medica, Chinese Academy of Sciences, Shanghai 201203, China
Correspondence: Jian-hua Shen (jhshen@simm.ac.cn) or Ying Leng (yleng@simm.ac.cn)

Received: 23 November 2022 Accepted: 15 March 2023
Published online: 30 March 2023

colitis [16]. However, no studies have investigated the role of TGR5 in regulating IEC apoptosis in the pathogenesis of UC until now, and the therapeutic effect of TGR5 agonist on UC has not yet been fully elucidated.

Here, we discovered OM8 as a novel potent and selective TGR5 agonist with high distribution in intestinal tract after oral administration, and demonstrated its therapeutic effect in DSS-induced murine colitis. More importantly, we identified a new mechanism of TGR5 agonist on inhibiting intestinal epithelial cells apoptosis through cAMP/PKA/c-FLIP/JNK signaling pathway.

MATERIALS AND METHODS

Animals

BALB/c mice (male, 20–22 g) and ICR mice (male, 26–28 g) were obtained from Shanghai Lingchang Biotechnology Co. (Shanghai, China). The animals were raised in the specific pathogen-free conditions with a controlled room temperature (22–24 °C) under 12 h light–dark cycles and had free access to food and water. All animal experiments were conducted with the approval of the Institutional Animal Care and Utilization Committee (IACUC) of Shanghai Institute of Materia Medica (SIMM), Chinese Academy of Sciences (CAS).

In vitro TGR5 and FXR activity assay

OM8 (purity >98.5%) and 26a [17] were synthesized by the laboratory of JHS, SIMM, CAS. HEK293 cells stably expressed with h/mTGR5 and CRE-driven luciferase reporter were generated and maintained as described [18]. The cells were seeded into 96-well plates. The next day, fresh medium containing different concentrations of OM8 was added and incubated for 5.5 h. Human FXR (hFXR) eukaryotic expression vector and reporter plasmid containing receptor response sequence were transferred into Huh7 cells to detect the agonistic activity of OM8 on FXR [19]. The Steady-Glo® Luciferase Assay System (Cat#E2510, Promega, Madison, WI, USA) and PerkinElmer Envision microplate reader were employed to detect the luciferase activity of cell lysates in accordance with the instructions of the manufacture.

Distribution of OM8 in intestinal tract and serum after single oral dose

OM8 (100 mg/kg) was orally administered to overnight-fasted ICR mice ($n = 6$ per time point). Different intestinal segments and blood samples were collected at 1, 2, 4, and 8 h after dosing. The concentrations of OM8 in the duodenum, jejunum, ileum, colon and serum were measured by LC-MS/MS.

Evaluation of gallbladder-filling effects

The ICR mice ($n = 6$–7 per group) were orally administered with OM8 (200 mg/kg) or 26a (100 mg/kg) for 3 days. The mice were fasted overnight before the last dose. At 1 h post dose, all mice were refed for 3 h and then dissected. The width and length of the gallbladder were measured using a Vernier caliper. The area of the gallbladder was calculated: area=length × width. Bile samples were then obtained and weighed.

Establishment of colitis mouse models and treatment

BALB/c male mice were assigned into four groups ($n = 10$) according to the body weight: normal group, DSS group, DSS + OM8 (50 mg/kg) group and DSS + OM8 (200 mg/kg) group. All animals except the normal group were given 3% (*w*/*v*) DSS (Cat#160110, MP Biomedicals, Irvine, CA, USA) in drinking water from day 0 to day 8, and then replaced with normal sterile drinking water on day 9. OM8 was mixed with polyvinyl pyrrolidone (PVP, Cat#30154480, Sinopharm Chemical Reagent Co., Shanghai, China) at 1:5 ratio and then diluted in sterile water. The mice were orally administered with OM8 (50 or 200 mg/kg) once daily or vehicle (1 g/kg PVP diluted in sterile water) throughout the experiment. Body weight, stool consistency and fecal occult blood were determined every day. Fecal occult blood test kit was bought from Nanjing Jiancheng Bioengineering Institute (Cat#C027-1-1, Nanjing, China). Disease activity index (DAI) scores of colitis was defined as previously described [20]. Mice were anesthetized with Zoletil (Virbac Laboratories, Carros, France) on day 9, and the colon and blood samples were collected.

Histological examination

The colonic segments were fixed in 10% (*v*/*v*) formaldehyde solution, embedded in paraffin, and sliced into 4 μm thickness paraffin sections. Subsequently, the sections were deparaffinized in xylene and rehydrated, followed by staining with Haematoxylin and Eosin (H&E) for histopathological observation or Alcian-Blue (AB) (Cat#G1560, Solarbio Life Sciences, Beijing, China) to evaluate the abundance of goblet cells. The images were acquired with five randomly selected fields in each section. The histological damage was blindly evaluated according to a scoring system by Ning et al at 200× magnification [21], taking account into inflammatory cell infiltration, mucosal and crypt injury.

Measurement of myeloperoxidase (MPO) activity

Briefly, the distal colons were homogenized in 0.5% (*w*/*v*) hexadecyltrimethylammonium bromide buffer (HTAB, Cat#57-09-0, Sinopharm Chemical Reagent Co., Shanghai, China, dissolved in 50 mM potassium phosphate buffer, pH = 6.0; 50 mg/mL tissue) and then centrifuged. Supernatants (7 μL) were added to 200 μL of 50 mM potassium phosphate buffer mixed with 0.167 mg/mL of *o*-dianisidine dihydrochloride and 0.05 μL of 1% (*v*/*v*) H_2O_2. Absorbance was measured at 450 nm using a spectrophotometer.

TUNEL assay

One Step TUNEL Apoptosis Assay Kit (Cat#MA0223, Meilunbio, Dalian, China) was used to assess the cell apoptosis in accordance with the manufacturer's instructions. Five random fields were photographed from each section, and the average number of TUNEL positive cells per field was calculated.

Immunohistochemical staining

Paraffin sections of colon tissue were dried at 60 °C, dewaxed by xylene, dehydrated by gradient alcohol, and pretreated with 3% (*v*/*v*) H_2O_2 for 10 min to quench endogenous peroxidase activity. Tissue sections were then boiled in 0.01 M citrate buffer (pH 6.0) by microwave heating for 10 min to facilitate antigen recovery and were then blocked with normal goat serum blocking solution at room temperature for 45 min. Subsequently, the sections were incubated with anti-F4/80 antibody (1:200, Cat#ab300421, Abcam, Cambridge, UK) and anti-CD11b antibody (1:200, Cat#ab133357, Abcam, Cambridge, UK) at 4 °C overnight. After rewarming for 30 min, sections were incubated for 1 h at room temperature with HRP-conjugated secondary antibody, stained with diaminobenzidine tetrahydrochloride (DAB, Cat#91-95-2, Sangon Biotech (Shanghai) Co., Ltd., Shanghai, China), and counterstained with Hematoxylin. Images were acquired using Leica DM 6B upright microscope.

Cell culture and treatment

Human colonic cell lines (HT-29 and Caco-2) were originated from American Type Culture Collection (ATCC, Manassas, VA, USA). HT-29 cells were cultured with McCoy's 5 A Modified Medium (Cat#16600082, Gibco, Grand Island, NY, USA) supplemented with 10% (*v*/*v*) fetal bovine serum (FBS, Cat#10099, Gibco, Grand Island, NY, USA) and 1% (*v*/*v*) penicillin-streptomycin. Caco-2 cells were cultured in Dulbecco's Modified Eagle's medium (DMEM) supplemented with 10% FBS, 1% (*v*/*v*) penicillin-streptomycin, 1% (*v*/*v*) glutamax and 1% (*v*/*v*) non-necessary amino acid. HT-29 cells or Caco-2 cells were treated with 20 ng/mL TNF-α (Cat#300-01 A,

Table 1. Primer sequences of qRT-PCR.

Gene	Primers
TGR5	F 5′-GAGCGTCGCCCACCACTAGG-3′
	R 5′-CGCTGATCACCCAGCCCCATG-3′
TGR5 (human)	F 5′-CTACCACCCAAGCAGCCAAA-3′
	R 5′-TGAGCTGGACGGATGCTCT-3′
TNF-α	F 5′-TATGGCCCAGACCCTCACA-3′
	R 5′-GGAGTAGACAAGGTACAACCCATC-3′
IL-6	F 5′-CCACTTCACAAGTCGGAGGCTTA-3′
	R 5′-GCAAGTGCATCATCGTTGTTCATAC-3′
IL-1β	F 5′-TCCAGGATGAGGACATGAGCAC-3′
	R 5′-GAACGTCACACACCAGCAGGTTA-3′
iNOS	F 5′-CGCTTGGGTCTTGTTCACTC-3′
	R 5′-GGTCATCTTGTATTGTTGGGCTG-3′
ZO-1	F 5′-AGGACACCAAAGCATGTGAG-3′
	R 5′-GGCATTCCTGCTGGTTACA-3′
Occludin	F 5′-TGGCAAGCGATCATACCCAGA-3′
	R 5′-CTGCCTGAAGTCATCCACACTC-3′
Claudin	F 5′-GGACTGTGGATGTCCTGCGTTT-3′
	R 5′-GCCAATTACCATCAAGGCTCGG-3′
GLP-2R	F 5′-TCATCTCCCTCTTCTTGGCTCTTAC-3′
	R 5′-TCTGACAGATATGACATCCATCCAC-3′
EGF	F 5′-TTCTCACAAGGAAAGAGCATCTC-3′
	R 5′-GTCCTGTCCCGTTAAGGAAAAC-3′
LGR5	F 5′-GTGGACTGCTCGGACCTG-3′
	R 5′-GCTGACTGATGTTGTTCATACTGAG-3′
Ascl2	F 5′-GTTAGGGGGCTACTGAGCAT-3′
	R 5′-GTCAGCACTTGGCATTTGGT-3′
Olfm4	F 5′-CAGCCACTTTCCAATTTCACTG-3′
	R 5′-GCTGGACATACTCCTTCACCTTA-3′
Mucin2	F 5′-ATGCCCACCTCCTCAAAGAC-3′
	R 5′-GTAGTTTCCGTTGGAACAGTGAA-3′
TFF3	F 5′-TAATGCTGTTGGTGGTCCTG-3′
	R 5′-CAGCCACGGTTGTTACACTG-3′
KLF4	F 5′-CCAAAGAGGGGAAGAAGGTC-3′
	R 5′-CTGTGTGAGTTCGCAGGTGT-3′
LYZ	F 5′-ATGGCGAACACAATGTCAAA-3′
	R 5′-GCGAGGAAGTGTGACCTCTC-3′
ChgA	F 5′-CCAAGGTGATGAAGTGCGTC-3′
	R 5′-GGTGTCGCAGGATAGAGAGGA-3′
CCL2	F 5′-TTTTTGTCACCAAGCTCAAGAG-3′
	R 5′-TTCTGATCTCATTTGGTTCCGA-3′
CXCL2	F 5′-CCCAGACAGAAGTCATAGCCAC-3′
	R 5′-GCCTTGCCTTTGTTCAGTATC-3′
GAPDH	F 5′-AGGTCGGTGTGAACGGATTTG-3′
	R 5′-TGTAGACCATGTAGTTGAGGTCA-3′

Peprotech, New Jersey, CT, USA) in the presence or absence of OM8 for 24 h. In some cases, adenylate cyclase (AC) inhibitor MDL-12330-A (3 μM) or protein kinase A (PKA) inhibitor H89 (5 μM) was added simultaneously with TNF-α and OM8.

Measurement of intestinal epithelial monolayer barrier in vitro
Caco-2 cells at the density of 3×10^5 cells/well were seeded in 24-well transwell chambers with 0.4 μm pore polyester membranes (Cat#3470, Corning Inc., Grand Island, NY, USA) and cultured for 21 days to form monolayer. The cells were treated with 20 ng/mL TNF-α and OM8 for 5 days, then the TEER values and permeability of FITC-dextran were determined.

RNA interference
The siRNA pool targeted to human TGR5 was obtained from Dharmacon (L-005519-00-0005, Lafayette, CO, USA). Three pairs of c-FLIP siRNA and negative control siRNA were provided by GenePharma (Shanghai, China). HT-29 cells were transfected with selective siRNA using Lipofectamine™ 2000 (Cat#11668027, Thermo Fisher Scientific, MA, USA) for 48 h according to the manufacture's illustration for the following experiments.

Immunofluorescence analysis
Paraffin sections of colon tissue were prepared as described in immunohistochemical staining. HT-29 cells were supplemented with 4% (*v*/*v*) paraformaldehyde and fixed for 30 min. Then the sections and cells were blocked with 3% (*w*/*v*) BSA (diluted in PBS) for 1 h at room temperature, and incubated with anti-Ki67 antibody (1:100, Cat#ab279653, Abcam, Cambridge, UK), anti-LGR5 antibody (1:50, Cat#abs120810, Absin Bioscience Inc., Shanghai, China), anti-LYZ antibody (1:100, Cat#ab108508, Abcam, Cambridge, UK), anti-ZO-1 antibody (1:200, Cat#13663, Cell Signaling Technology, Boston, MA, USA) and anti-Occludin antibody (1:200, Cat#ab216327, Abcam, Cambridge, UK) at 4 °C overnight, followed by FITC goat anti-rabbit IgG (H + L) secondary antibody (1:100, AS011, ABclonal Technology, Wuhan, China), Cy3 goat anti-mouse IgG (H + L) secondary antibody (1:100, AS008, ABclonal Technology, Wuhan, China) and donkey anti-rabbit IgG (H + L) highly cross-adsorbed secondary antibody (1:500, Cat#A-31572, Thermo Fisher Scientific, Waltham, CA, USA) incubation for 60 min. The nucleus was counterstained with DAPI (Cat#C1002, Beyotime, Shanghai, China) for 2 min, sealed with anti-fluorescence quenching agent. The images were obtained under a Leica two-photon microscopy.

RNA and Quantitative RT-PCR
Total RNA of colon tissues and cells was extracted using TRIzol reagent (Thermo Fisher Scientific, Waltham, CA, USA) and the RNA concentration was determined. Total RNA was reversely transcribed into complementary DNA (cDNA) by a Primer Script RT reagent kit (TaKaRa Biotechnology, Dalian, China). Quantitative RT-PCR was performed in CFX96 real-time PCR detection (Bio-Rad, Hercules, CA, USA) systems using SYBR Premix Ex Taq kit (Takara Biotechnology, Dalian, China). All of the primer sequences used in our study were synthesized by Thermo Fisher Scientific Co., Ltd., (Waltham, CA, USA) as shown in Table 1. Relative mRNA expression of individual gene was normalized against GAPDH.

Western blot analysis
The tissues and cells were lysed with lysis buffer. The protein concentration was measured and adjusted by adding the appropriate amount of 5× loading buffer. Then the lysates were boiled for 15 min to denature the protein. After centrifugation, the proteins were separated by 10% (*v*/*v*) sodium dodecyl sulfate-polyacrylamide gel electrophoresis gels (SDS-PAGE) and wet-transferred onto the polyvinylidene fluoride (PVDF) membrane. The membrane was blocked and incubated with primary antibodies at 4 °C overnight, and then incubated with HRP-conjugated secondary antibody (Bio-Rad, Hercules, CA, USA) for 2 h. Chemiluminescence (ECL) working solution (GE Healthcare, Buckinghamshire, UK) was used for protein detection, and the quantification analysis was performed using the Quality One software (Bio-Rad, Hercules, CA, USA). The primary antibodies against ZO-1 (Cat#13663), phospho-CREB (Ser133) (Cat#9198), CREB (Cat#9197), cleaved caspase-3 (Cat#9664), p-JNK (Cat#4668), p-JNK (Cat#9252), p-p38 (Cat#9211), c-FLIP (Cat#8510), GAPDH (Cat#5174) and β-actin (Cat#4970) were purchased from Cell Signaling Technology (Boston, MA, USA). The primary antibody

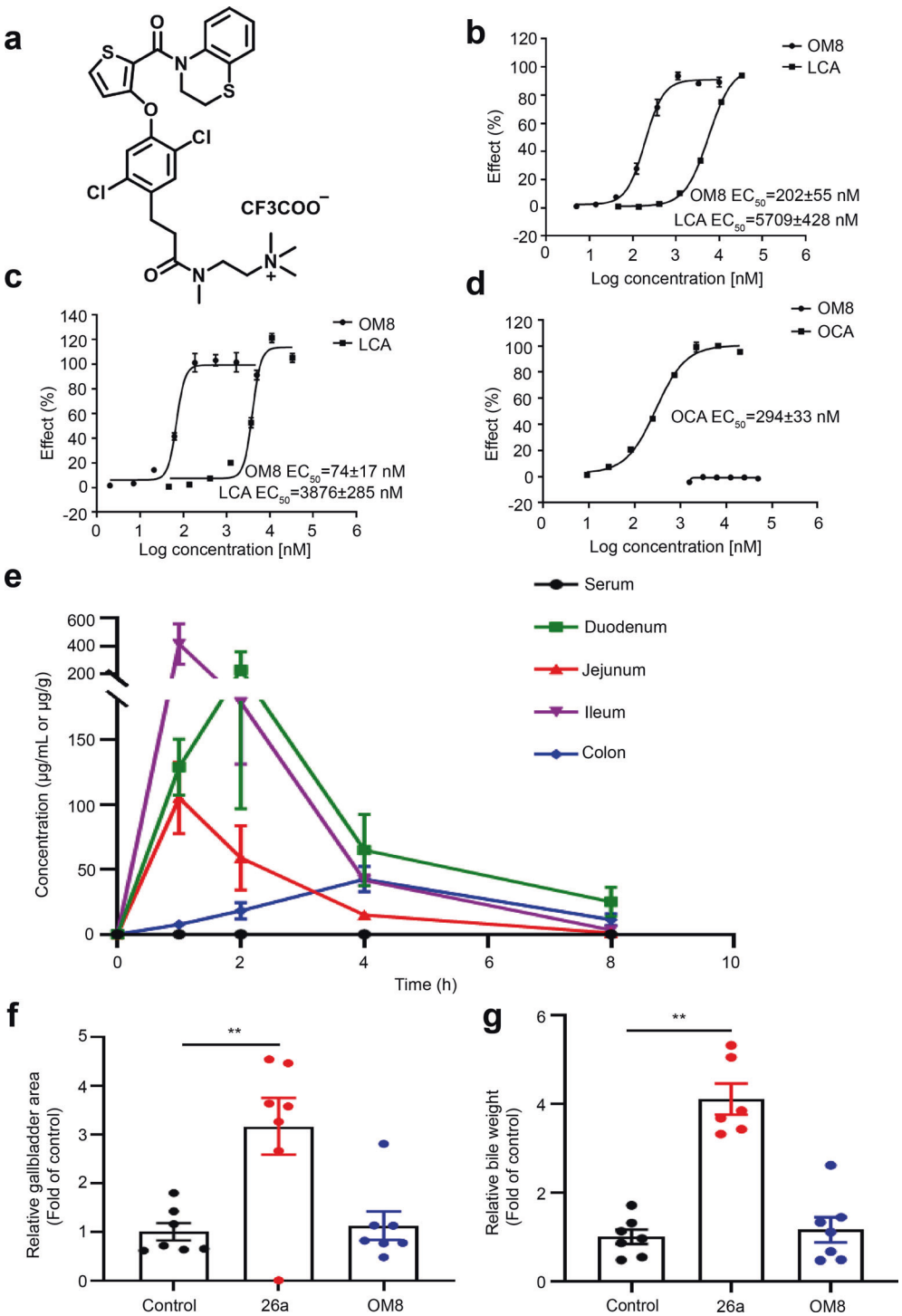

Fig. 1 OM8 is a potent and selective TGR5 agonist. a Chemical structure of compound OM8. **b** Activation effect of OM8 on hTGR5. **c** Activation effect of OM8 on mTGR5. **d** Activation effect of OM8 on hFXR. **e** Concentrations of OM8 in serum, duodenum, jejunum, ileum and colon. **f** Gallbladder area. **g** Bile weight. Data are presented as mean ± SD ($n = 3–7$). $^{**}P < 0.01$.

against Occludin (Cat#ab216327) was bought from Abcam (Cambridge, UK).

Statistical analysis

The statistical analysis was fulfilled using GraphPad Prism 8.0 software. All the data were displayed as mean ± standard deviation. One-way analysis of variance (ANOVA) was applied to compare data among multiple groups followed by Dunnett's or Tukey's *post hoc* test. $P < 0.05$ indicated significant difference.

RESULTS

OM8 is a potent and selective TGR5 agonist with high distribution in intestinal tract

In this study, we generated a novel TGR5 agonist OM8 (Fig. 1a). This small molecule exhibited potent activity with EC_{50} values of 202 ± 55 nM on hTGR5 and 74 ± 17 nM on mTGR5, which was much more active than LCA, the natural ligand of TGR5 (Fig. 1b, c). Moreover, OM8 showed no agonistic activity on hFXR, whereas the FXR agonist obeticholic acid (OCA) activated hFXR with an

Table 2. Concentrations of OM8 in serum and intestinal tract at different time points after oral administration.

	0 h	1 h	2 h	4 h	8 h
Serum (μg/mL)	BLQ	0.14	0.10	0.03	0.01
Duodenum (μg/g)	BLQ	128.86	227.68	64.99	25.12
Jejunum (μg/g)	BLQ	105.09	58.95	15.00	1.16
Ileum (μg/g)	BLQ	415.17	178.74	41.75	3.31
Colon (μg/g)	BLQ	7.51	18.19	42.52	11.34

BLQ Below limit quantification.

EC_{50} value of 294 ± 33 nM (Fig. 1d). The concentration of OM8 in serum and intestinal tract at 1, 2, 4, 8 h post dose was examined in mice with an oral dose of 100 mg/kg. As shown in Fig. 1e and Table 2, the serum concentration of OM8 reached 0.14 μg/mL at 1 h, and then fell to 0.01 μg/mL at 8 h post dose. The concentration of OM8 at 1 h post dose in intestinal tissue was relatively high, with 128.86, 105.09, 415.17, 7.51 μg/g in duodenum, jejunum, ileum and colon, respectively. And the level of OM8 in colon was still kept as 11.34 μg/g even at 8 h post dose. The results indicated that the absorption of OM8 in the blood was quite low, and a large amount of OM8 was maintained in intestinal tract after oral administration. Then, the effect of OM8 on gallbladder filling was examined in ICR mice. 26a, a previous reported TGR5 agonist with gallbladder-filling effects [17], was utilized as positive control here. As shown in Fig. 1f, g, 26a significantly increased gallbladder area and bile weight compared with control group, while OM8 showed no significant impact on gallbladder area and bile weight, demonstrating that OM8 can effectively avoid gallbladder side effects. Therefore, OM8 was a potent and selective TGR5 agonist with high distribution in intestinal tract.

OM8 attenuated DSS-induced colitis

The mice were challenged with 3% DSS to establish DSS-induced colitis model, and the protective effect of OM8 on colitis was evaluated. During the experimental process, all mice survived and mice in DSS group developed severe weight loss, diarrhea and stool occult blood, 50 and 200 mg/kg OM8 significantly improved these alterations and decreased DAI scores (Fig. 2a). Meanwhile, the shortened colon length and increased colon weight/length ratio caused by DSS were also ameliorated by OM8 (Fig. 2b–d). H&E staining revealed that OM8 treatment significantly attenuated inflammatory cell infiltration and retained more intact crypt architecture in the colon of DSS-induced mice (Fig. 2e, f). Notably, a decreased mRNA level of TGR5 was observed in the colon of DSS-induced mice, which was remarkably recovered by OM8 treatment (Fig. 2g). OM8 administration significantly reduced colonic MPO activity, decreased the mRNA levels of proinflammatory cytokines iNOS and TNF-α, and the gene expression of IL-1β and IL-6 also showed decreased tendency (Fig. 2h–l). The elevated gene expression of chemokines CCL2 and CXCL2 caused by DSS was also significantly abrogated (Fig. 2m, n). Moreover, the hyperinfiltration of immune cells was restrained by OM8 treatment, as evidenced by decreased immunostaining of F4/80 and CD11b in colon sections (Fig. 2o). Therefore, OM8 could ameliorate the DSS-induced colitis.

OM8 restored tight junction proteins expression in DSS-induced colitis mice

Tight junction proteins are important components of intestinal epithelial barrier. The colonic mRNA expression of ZO-1, Occludin and Claudin were significantly decreased in DSS-induced colitis, but could be restored by OM8 intervention (Fig. 3a–c). Moreover, OM8 also significantly increased ZO-1 and Occludin protein expression in the colon of DSS-treated mice (Fig. 3d). Immunofluorescence staining showed that ZO-1 and Occludin were distributed orderly and completely in colon of normal mice, while the obvious deficiency was observed in DSS-treated mice, and OM8 treatment significantly maintained the intact distribution of ZO-1 and Occludin (Fig. 3e, f). These data suggested that OM8 could restore tight junction proteins expression and distribution in DSS-induced colitis mice.

OM8 drove ISCs proliferation and differentiation in DSS-induced colitis mice

Ordinated intestinal stem cell proliferation and differentiation was essential for maintaining intestinal epithelial barrier function. Immunofluorescence analyses showed that OM8 treatment significantly reversed the sharp decrease of $Ki67^+$ cells in the colonic epithelium caused by DSS (Fig. 4a, b). Meanwhile, the loss of $LGR5^+$ ISCs in the colon crypt caused by DSS was improved by OM8, and a higher amount of $LGR5^+Ki67^+$ cells was noticed in the colon crypt of colitis mice after OM8 administration (Fig. 4c, d). Though no obvious change of Olfm4 gene expression was observed, the mRNA levels of the other two intestinal stem cell marker gene LGR5 and Ascl2 were significantly enhanced in the colon of DSS-induced colitis mice after OM8 intervention (Fig. 4e–g). Moreover, OM8 administration obviously increased the gene expression of goblet cell marker (Mucin2, TFF3 and KLF4), Paneth cell marker LYZ and enteroendocrine cell-associated marker ChgA in the colon of colitis mice (Fig. 4h–l). Alcian Blue (AB) staining analysis showed that DSS led to tremendous loss of goblet cells, and this effect could be markedly reversed by OM8 treatment (Fig. 4m). Immunofluorescence labeling for Lysozyme showed that OM8 obviously preserved the number of LYZ-positive cells in the colon of colitis mice (Fig. 4n). These results suggested that OM8 treatment could promote intestinal stem cell proliferation and differentiation in DSS-induced colitis.

OM8 inhibited intestinal epithelial cell apoptosis both in vivo and in vitro

Excessive intestinal cell apoptosis is related to the destruction of intestinal epithelial barrier function. As shown in Fig. 5a, b, the TUNEL-positive cells were obviously increased in the colonic epithelium of DSS-induced colitis mice, and OM8 treatment significantly decreased the rate of TUNEL-positive cells, suggesting that OM8 might reduce intestinal epithelial cell apoptosis in DSS-induced colitis mice. Meanwhile, the enhanced protein expression of cleaved caspase-3 in DSS-induced colitis was apparently suppressed with OM8 treatment (Fig. 5c).

TNF-α was the key driver of cell apoptosis in intestinal tissue of IBD patients. To investigate whether OM8 has a direct effect on intestinal epithelial cell apoptosis, HT-29 cells and Caco-2 cells were incubated with TNF-α to induce apoptosis in vitro. As shown in Fig. 5d, the proportion of TUNEL-positive cells was markedly increased upon TNF-α incubation in HT-29 cells, and this effect could be blocked by OM8 treatment. The enhanced protein expression of cleaved caspase-3 induced by TNF-α was significantly abolished by OM8 treatment in HT-29 cells (Fig. 5e). Meanwhile, OM8 treatment could also reduce the increased protein expression of cleaved caspase-3 caused by TNF-α in Caco-2 cell (Fig. 5f). Then, the effects of OM8 on TNF-α-induced Caco-2 monolayer damage were determined. As shown in Fig. 5g, OM8 treatment significantly increased the impaired TEER value of Caco-2 monolayers induced by TNF-α. Meanwhile, the increased permeability of FITC-dextran in Caco-2 monolayers caused by TNF-α was also significantly reduced by OM8 (Fig. 5h). The above results suggested that OM8 inhibited TNF-α induced intestinal

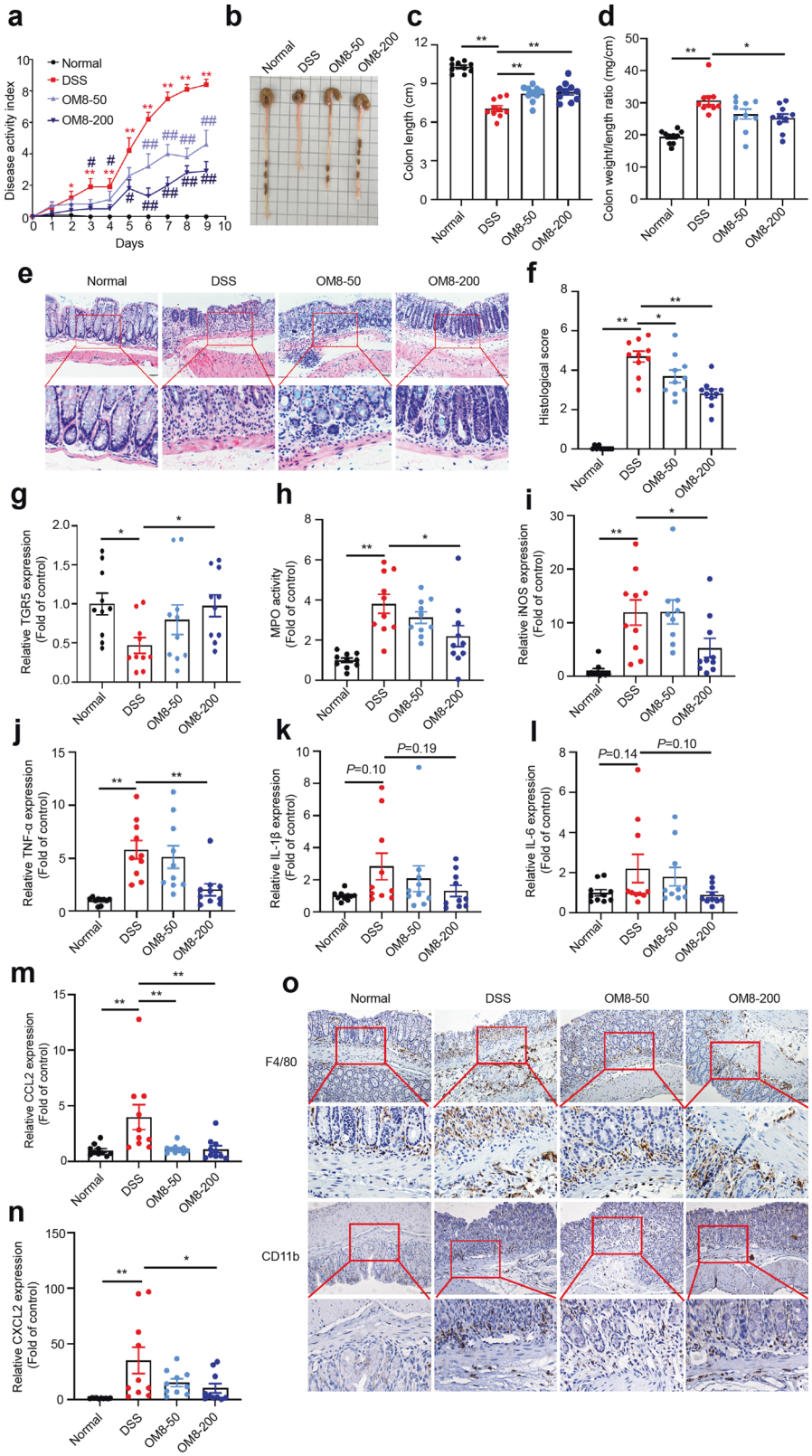

Fig. 2 OM8 could attenuate DSS-induced colitis. **a** DAI score. **b** Representative photograph of colon. **c** Colon length. **d** Colon weight/length ratio. **e** Representative H&E staining images in colon sections, Bar = 50 μm. **f** Histological score. **g** Relative mRNA levels of TGR5 in colon. **h** MPO activity. Relative mRNA levels of inflammatory cytokines iNOS (**i**), TNF-α (**j**), IL-1β (**k**), IL-6 (**l**), CCL2 (**m**) and CCXL2 (**n**) in colon. **o** Representative images of immunohistochemistry staining for F4/80 and CD11b in colon sections, Bar = 50 μm. Data are presented as mean ± SD ($n = 9$–10). **a** $^{*}P < 0.05$; $^{**}P < 0.01$ compared with the normal group; $^{\#}P < 0.05$; $^{\#\#}P < 0.01$ compared with the DSS group. **c**–**n** $^{*}P < 0.05$; $^{**}P < 0.01$.

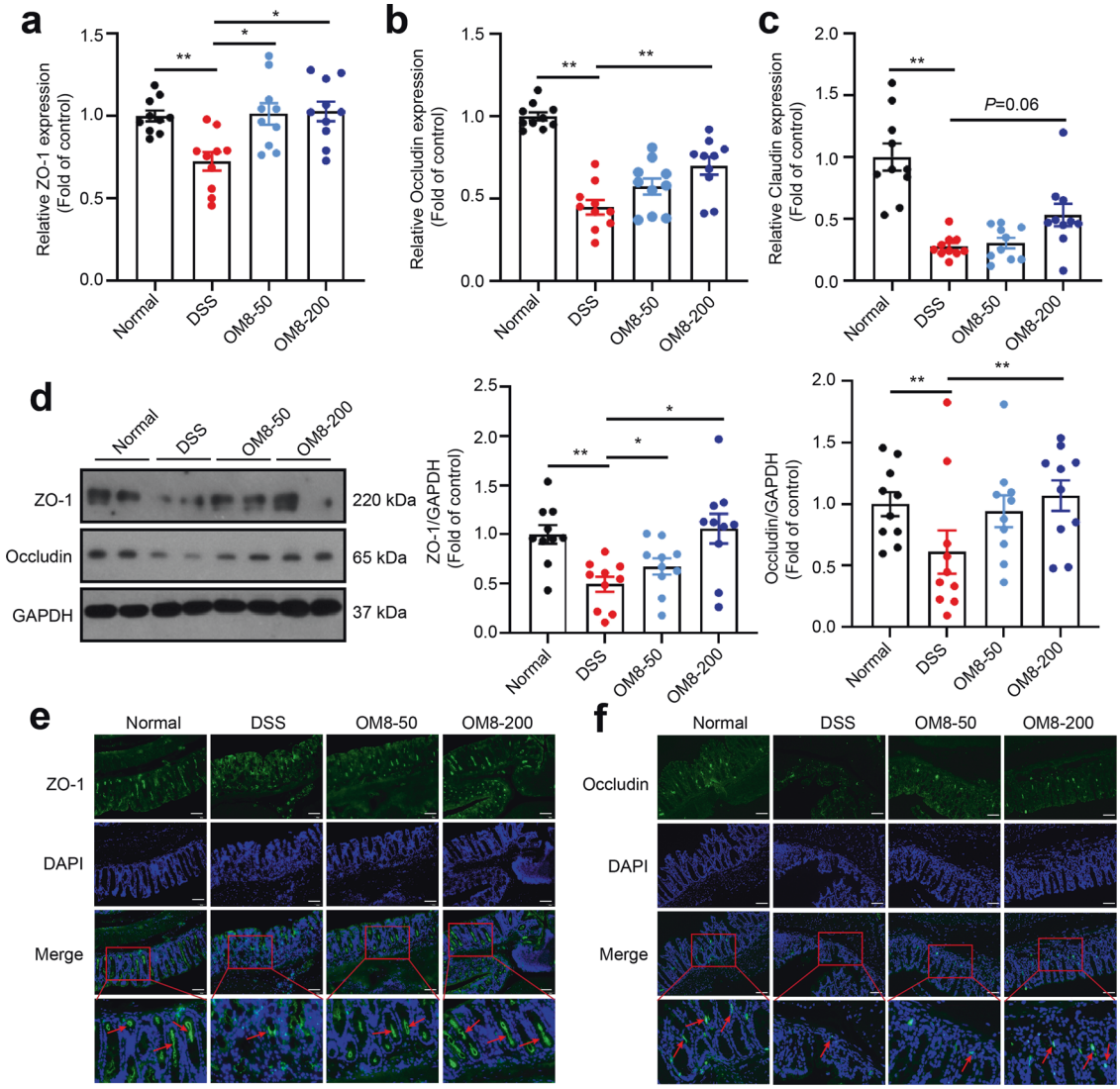

Fig. 3 OM8 restored tight junction proteins expression in DSS-induced colitis mice. Relative mRNA levels of tight junction proteins ZO-1 (**a**), Occludin (**b**) and Claudin (**c**) in colon. **d** Relative protein levels of ZO-1 and Occludin in colon. **e** Colon sections were immunostained with ZO-1 (green) and DAPI (blue), Bar = 50 μm. **f** Colon sections were immunostained with Occludin (green) and DAPI (blue), Bar = 50 μm. Data are presented as mean ± SD ($n = 10$). *$P < 0.05$; **$P < 0.01$.

epithelial cell apoptosis and improved the intestinal epithelial monolayer barrier dysfunction.

OM8 suppressed TNF-α induced intestinal epithelial cell apoptosis in a TGR5-dependent manner

In order to explore the involvement of TGR5 in the inhibition by OM8 on TNF-α induced intestinal epithelial cell apoptosis, TGR5 RNAi was conducted in HT-29 cells. As shown in Fig. 6a, both TNF-α and OM8 treatment had no effect on the gene expression of TGR5 in HT-29 cells, which was significantly decreased by transfection with siRNA targeting TGR5. TUNEL staining showed that silencing TGR5 completely blocked the inhibition by OM8 on TNF-α induced apoptosis in HT-29 cells (Fig. 6b). Meanwhile, the suppression of TNF-α induced cleaved caspase-3 protein expression by OM8 was totally vanished in TGR5-deficient HT-29 cells (Fig. 6c). Furthermore, immunofluorescence staining showed that OM8 improved the disruption of ZO-1 protein expression and distribution induced by TNF-α, while knockdown of TGR5 interrupted the restoration of ZO-1 protein expression and distribution by OM8 (Fig. 6d). Collectively, these data demonstrated that OM8 prevented TNF-α induced intestinal epithelial cell apoptosis in a TGR5-dependent manner.

OM8 inhibited TNF-α induced JNK phosphorylation in intestinal epithelial cells through TGR5/cAMP/PKA signaling pathway

Activation of JNK pathway is closely related to the initiation and acceleration of TNF-α induced cell apoptosis [22–25]. Besides, p38 MPAK signaling may also be involved in cell apoptosis stimulated by TNF-α [24, 25]. As shown in Fig. 7a, TNF-α dramatically increased JNK phosphorylation in HT-29 cells, and this effect could be significantly compromised by OM8 treatment. Meanwhile, OM8 showed no effect on TNF-α induced p38 phosphorylation in HT-29 cells (Fig. 7b). Furthermore, transfection with siRNA targeting TGR5 abolished the inhibition by OM8 on TNF-α induced JNK phosphorylation in HT-29 cells (Fig. 7c), suggesting that activation of TGR5 is indispensable for the inhibition by OM8 on TNF-α induced JNK phosphorylation. As a selective TGR5 agonist, OM8 significantly elevated intracellular cAMP levels in HT-29 cells (Fig. 7d). Then, AC inhibitor MDL-12330-A and PKA inhibitor H89 were employed to ascertain whether TGR5/cAMP/PKA axis is involved in the inhibition by OM8 on TNF-α induced JNK phosphorylation in HT-29 cells. As shown in Fig. 7e, the suppression of TNF-α induced JNK phosphorylation and apoptosis induced by OM8 was entirely blocked by MDL-12330-A.

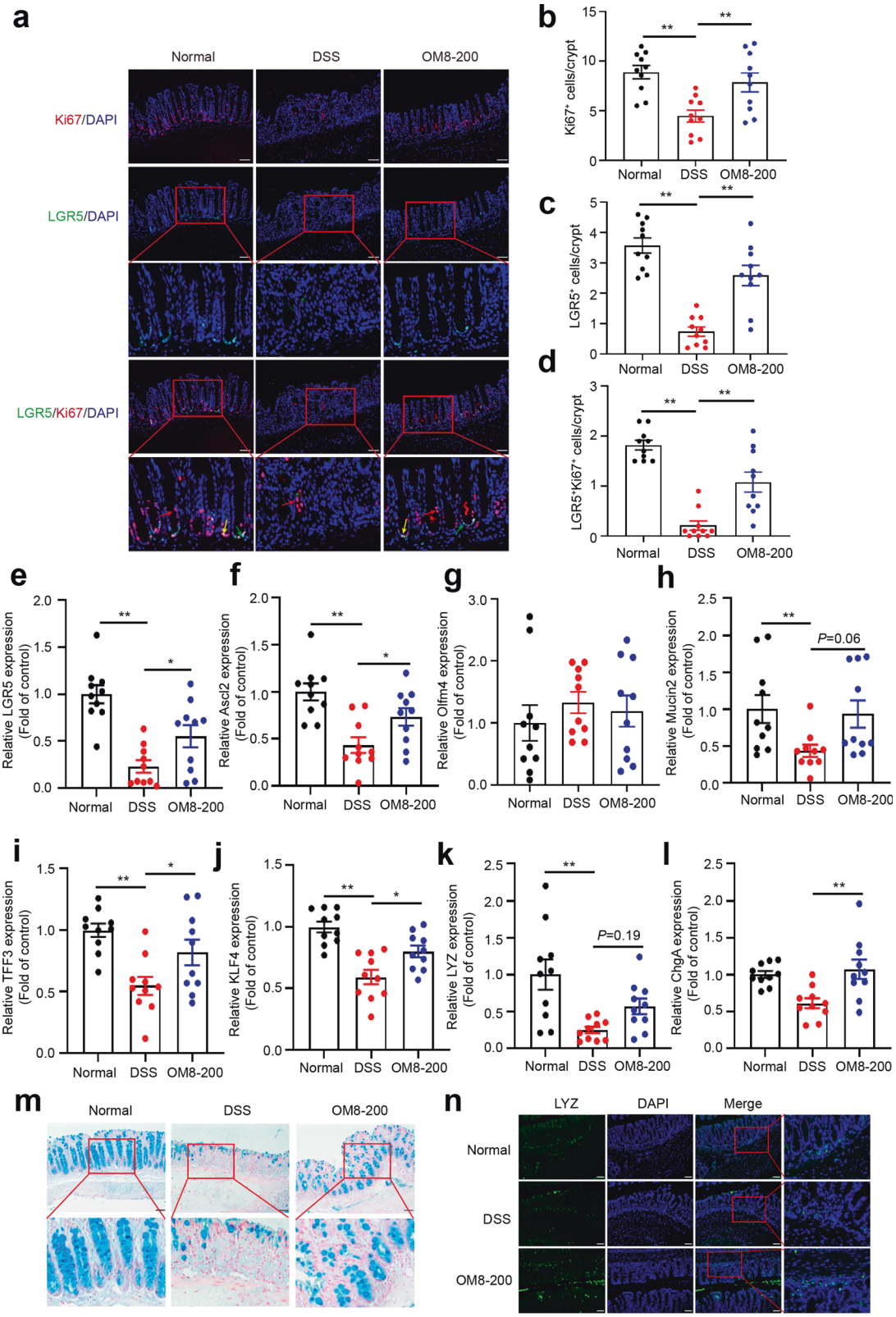

Fig. 4 OM8 drove ISCs proliferation and differentiation in DSS-induced colitis mice. a Colon sections were immunostained with Ki67 (red), LGR5 (green) and DAPI (blue), Bar = 50 μm, red arrows indicated $Ki67^+$ cells, green arrows indicated $LGR5^+$ ISCs and yellow arrows indicated $LGR5^+Ki67^+$ cells. **b** Quantitative result of immunofluorescence staining for $Ki67^+$ cells. **c** Quantitative result of immunofluorescence staining for $LGR5^+$ ISCs. **d** Quantitative result of immunofluorescence staining for $LGR5^+Ki67^+$ cells. Relative mRNA levels of intestinal stem cell markers LGR5 (**e**), Ascl2 (**f**) and Olfm4 (**g**) in colon. Relative mRNA levels of goblet cell markers Mucin2 (**h**), TFF3 (**i**) and KLF4 (**j**) in colon. **k** Relative mRNA level of Paneth cell marker Lysozyme (LYZ) in colon. **l** Relative mRNA level of enteroendocrine cell marker ChgA in colon. **m** Representative alcian blue staining images in colon sections, Bar = 50 μm. **n** Colon sections were immunostained with LYZ (green) and DAPI (blue), Bar = 50 μm. Data are presented as mean ± SD ($n = 10$). *$P < 0.05$; **$P < 0.01$.

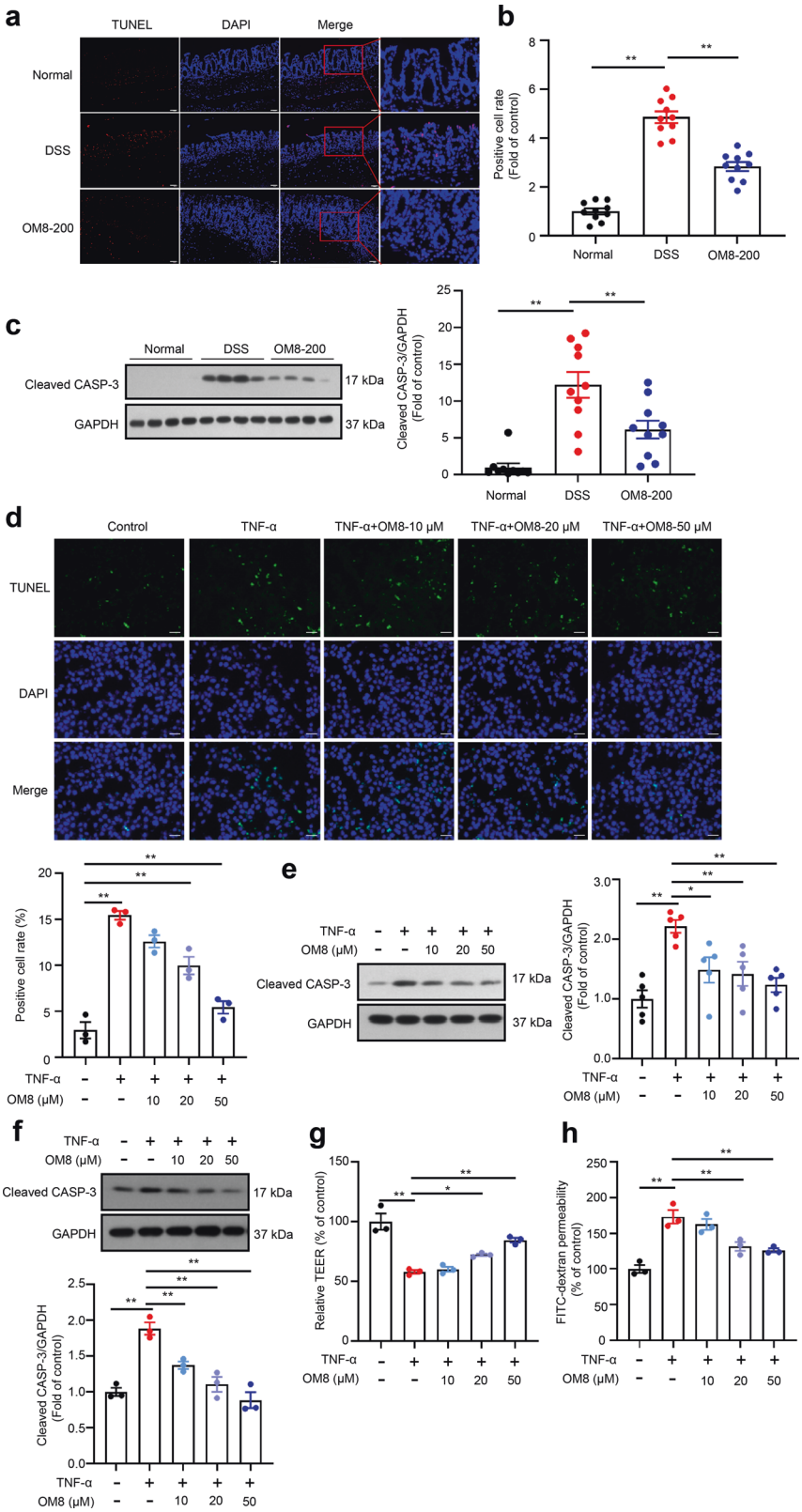

Consistently, H89 fully vanished the inhibition by OM8 on TNF-α induced JNK phosphorylation and apoptosis in HT-29 cells (Fig. 7f). These results revealed that OM8 inhibited TNF-α induced JNK phosphorylation through TGR5/cAMP/PKA signaling pathway in intestinal epithelial cells.

Upregulation of c-FLIP expression by TGR5/cAMP/PKA axis is indispensable for the inhibition by OM8 on TNF-α induced JNK phosphorylation and apoptosis in intestinal epithelial cells

c-FLIP is one of the main mediator in regulating TNF-α induced apoptosis. OM8 dose-dependently elevated the protein

Fig. 5 OM8 inhibited intestinal epithelial cell apoptosis both in vivo and in vitro. BALB/c mice were fed with 3% DSS in drinking water and orally administered with OM8 (200 mg/kg) or vehicle. The colon samples were collected on day 9. **a** Section of colon was subjected to TUNEL staining, Bar = 50 μm. **b** Quantitative result of TUNEL staining. **c** The protein levels of cleaved caspase-3 in colon. HT-29 cells were treated with or without 20 ng/mL TNF-α in the presence or absence of OM8 with the indicated concentrations for 24 h. **d** Apoptotic cells was analyzed by TUNEL staining, Bar = 50 μm. **e** Cleaved caspase-3 expression was determined by immunoblot assay. **f** Caco-2 cells were treated with or without 20 ng/mL TNF-α in the presence or absence of OM8 with the indicated concentrations for 24 h, cleaved caspase-3 expression was determined by immunoblot assay. Caco-2 cell monolayers were treated with or without 20 ng/mL TNF-α in the presence or absence of OM8 for 5 days. **g** The TEER value was determined. **h** FITC-dextran permeability was measured. Data are presented as mean ± SD (a–c: $n = 10$; d–h: $n = 3–5$). $^{*}P < 0.05$; $^{**}P < 0.01$.

expression of c-FLIP in HT-29 cells (Fig. 8a). To further investigate the role of c-FLIP in the inhibition by OM8 on TNF-α induced JNK phosphorylation and apoptosis, the RNAi was applied in HT-29 cells. As shown in Fig. 8b, the expression of c-FLIP protein was decreased with c-FLIP siRNA transfection and si-c-FLIP-3 with the highest silencing efficiency was chosen for subsequent experiments. With the knockdown of c-FLIP protein expression in HT-29 cells, the suppression of TNF-α induced JNK phosphorylation induced by OM8 was rescued (Fig. 8c). TUNEL staining showed that the inhibition by OM8 on TNF-α induced apoptosis was abrogated by silencing c-FLIP (Fig. 8d). Accordingly, the suppression of TNF-α induced cleaved caspase-3 protein expression induced by OM8 was also blocked in c-FLIP-deficient cells (Fig. 8e). Meanwhile, the restoration of TNF-induced damage to ZO-1 protein expression and distribution in HT-29 cells by OM8 was reversed by silencing c-FLIP (Fig. 8f). These data indicated that c-FLIP was indispensable for the inhibition by OM8 on TNF-α induced JNK phosphorylation and apoptosis in intestinal epithelial cells.

Then, further study was conducted to clarify the involvement of TGR5/cAMP/PKA axis in the upregulation of c-FLIP protein expression induced by OM8. As shown in Fig. 8g, silencing TGR5 interrupted the promotion effect of OM8 on c-FLIP protein expression in HT-29 cells. In addition, the enhancement of c-FLIP protein expression by OM8 was abolished by simultaneous treatment with MDL-12330-A or H89 (Fig. 8h, i), accompanied with the same change of CREB phosphorylation, indicating that OM8 promoted c-FLIP protein expression through TGR5/cAMP/PKA signaling pathway. The above results were further verified in vivo. As shown in Fig. 8j, OM8 administration significantly increased the levels of CREB phosphorylation and c-FLIP protein expression in the colon of DSS-treated mice. Meanwhile, the enhanced JNK phosphorylation induced by DSS was obviously inhibited by OM8 intervention. Taken together, these data suggested that OM8 upregulated c-FLIP protein expression through TGR5/cAMP/PKA signaling pathway, then suppressed JNK phosphorylation, and thereby inhibited TNF-α induced apoptosis in intestinal epithelial cells.

DISCUSSION

Breakdown of intestinal epithelial homeostasis characterized by uncoordinated ISC proliferation and IEC apoptosis is recognized as a hallmark of the UC pathophysiology [26–29]. While activation of TGR5 has been reported to facilitate ISC proliferation and crypts growth [16, 30], its role in IEC apoptosis remains unknown. Moreover, the beneficial effects of TGR5 agonist for the treatment of UC also need to be further evaluated. Here, we reported that a potent and selective TGR5 agonist OM8 could ameliorate DSS-induced colitis, which was mediated by the maintenance of intestinal epithelial homeostasis through reducing IEC apoptosis and promoting ISC proliferation. More importantly, the direct inhibition by OM8 on TNF-α induced IEC apoptosis with a TGR5-dependent manner was demonstrated in vitro, and a novel mechanism of TGR5 agonist on inhibiting IEC apoptosis through cAMP/PKA/c-FLIP/JNK signaling pathway was unraveled.

Although a few studies indicated that the activation of TGR5 might play a role in the prevention of colitis, the direct evidence from selective TGR5 agonists is still lacking. Hyodeoxycholic acid (HDCA) showed protective effects in DSS-induced colitis, but the involvement of FXR cannot be ruled out since HDCA is a non-selective TGR5 agonist [31]. Genistein might ameliorate the DSS-induced murine colitis by inhibition of NLRP3 inflammasome in macrophages through TGR5/cAMP signaling pathway, but the direct activation by genistein on TGR5 was absent [32]. Betulinic acid could ameliorate the DSS-induced murine colitis partially by activating TGR5 and stimulating GLP-2 secretion [33], but as a naturally occurring compound, the TGR5-independent activities including anti-inflammatory effect and FXR activation might also be involved [34]. In the present study, OM8, a novel potent and selective TGR5 agonist was generated. More importantly, the serum concentration of OM8 was quiet low, and a large amount of OM8 could be maintained in intestinal tract after oral administration, indicating that this compound might be more ascendant for the treatment of UC due to the persistent stimulation on TGR5 in the gut. Moreover, OM8 showed no significant impact on gallbladder area and bile weight, demonstrating that OM8 can effectively avoid gallbladder side effects. Oral treatment with OM8 relieved the weight loss, diarrhea, occult blood symptoms and shortening of colon length in DSS-induced colitis mice. Colonic mucosal inflammation, ulceration and architectural distortion, which are the major pathophysiological characteristics of colitis [35], were improved by OM8 treatment. In addition, OM8 administration dramatically reversed the impaired colonic expression of TJ proteins, which strengthened the finding concerning the modulation effect of TGR5 on TJ proteins expression [15], and indicated that the activation of TGR5 could improve intestinal epithelial barrier dysfunction in DSS-induced colitis. These findings suggested OM8, a potent and selective TGR5 agonist, could effectively attenuated DSS-induced colitis.

Extensive evidences have indicated that excessive IEC apoptosis contributes to the development of UC by augmenting intestinal permeability and amplifying inflammatory response [36, 37]. IEC apoptosis and enterocyte proliferation are tightly regulated. The continuous self-renewal of intestinal epithelium was impaired in UC progression, which is not only caused by aberrant apoptosis at the villous tip but also resulted from stunted enterocyte proliferation within the crypts, ultimately leading to imbalanced intestinal epithelial homeostasis and barrier dysfunction [33, 34]. Recently, lithocholic acid was reported to foster intestinal organoid proliferation through TGR5 [16]. In addition, activation of TGR5 in enteroendocrine L cells increased the release of GLP-2, which could also stimulate ISC proliferation [30]. Despite TGR5 activation has been reported to suppress apoptosis in multiple cells such as neurons and cholangiocytes [38, 39], its direct effect on IEC apoptosis is still unknown. Here, OM8 treatment significantly elevated the proliferating cell marker Ki67 [40] and ISC marker LGR5 [41] levels and increased the number of $LGR5^{+}Ki67^{+}$ cells in colon of DSS-induced colitis mice, suggesting that OM8 could promote ISC proliferation. Moreover, reduction of gene expression of various functional IECs markers induced by DSS, including goblet cells, paneth cells and enteroendocrine cells,

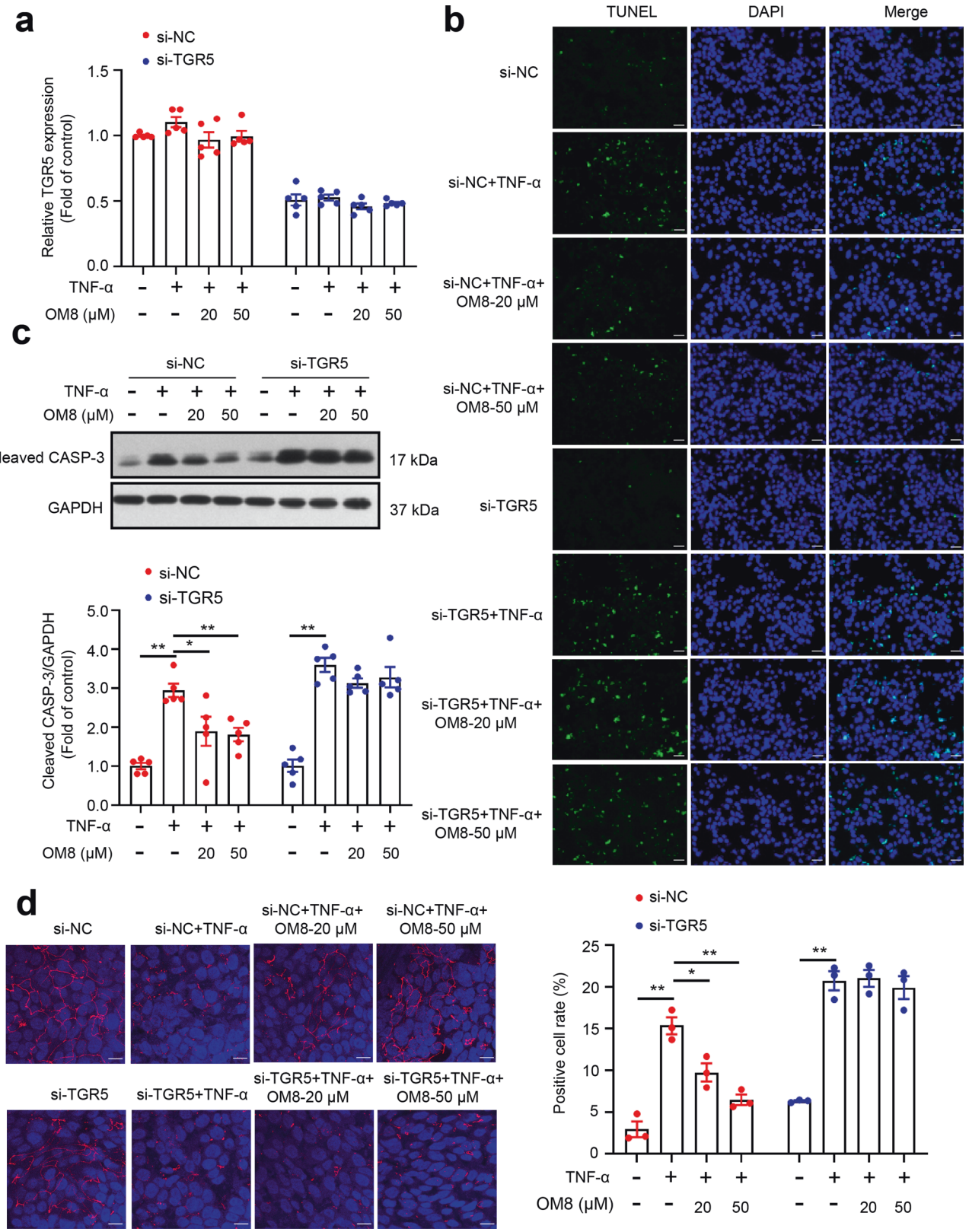

Fig. 6 OM8 suppressed intestinal epithelial cell apoptosis in a TGR5-dependent manner. HT-29 cells were transfected with TGR5 siRNA for 48 h and then treated with or without TNF-α in the presence or absence of OM8 for 24 h. **a** The efficiency of TGR5 siRNA was verified by RT-PCR. **b** Apoptotic cells were analyzed by TUNEL staining, Bar = 50 μm. **c** Cleaved caspase-3 expression was determined by immunoblot assay. **d** Confocal microscopy visualization of ZO-1 (red) and DAPI (blue), Bar = 10 μm. Data are presented as mean ± SD ($n = 3$–5). $^{*}P < 0.05$; $^{**}P < 0.01$.

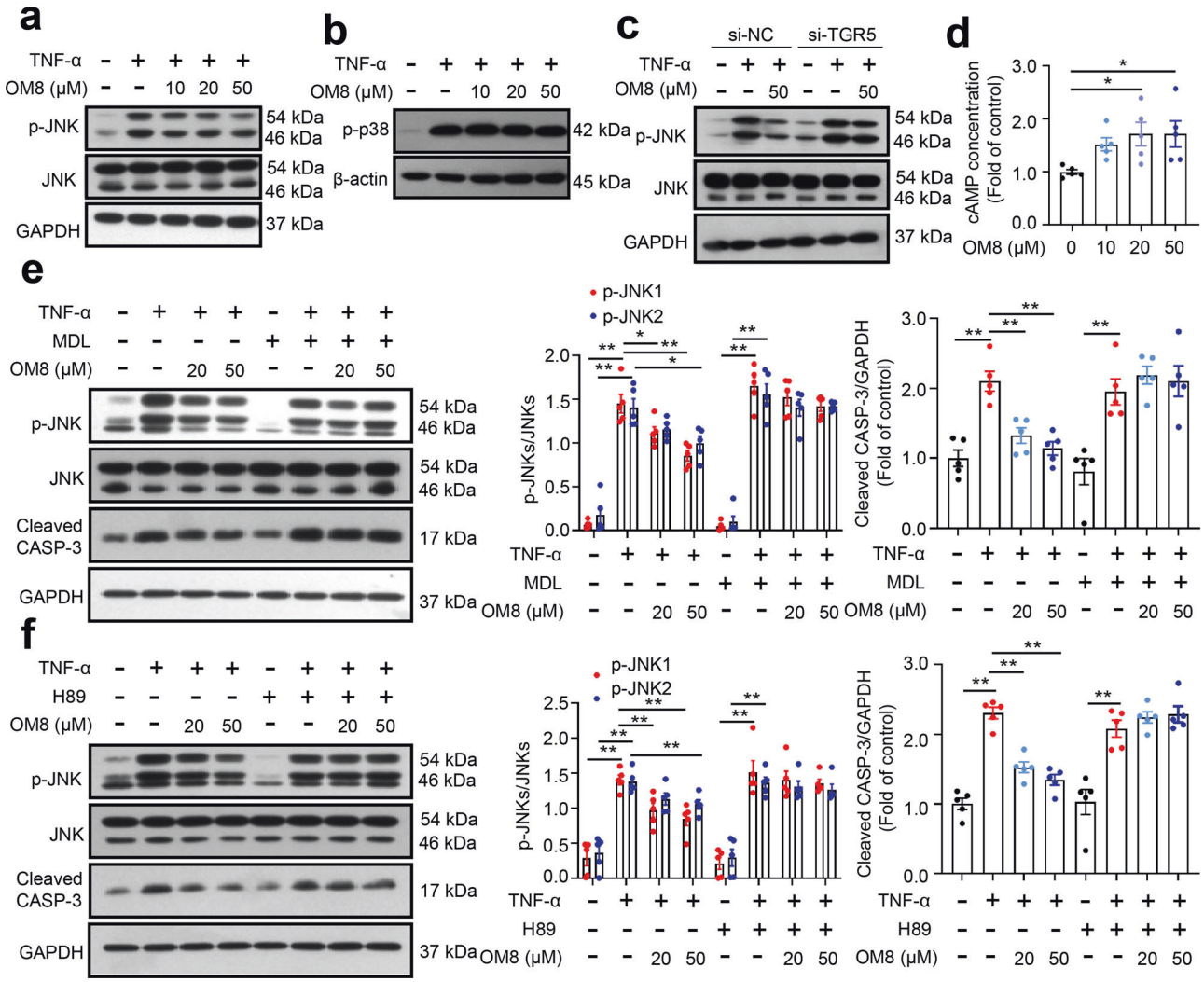

Fig. 7 OM8 inhibited TNF-α induced JNK phosphorylation in intestinal epithelial cells through TGR5/cAMP/PKA signaling pathway. **a**, **b** HT-29 cells were treated with or without 20 ng/mL TNF-α in the presence or absence of OM8 with the indicated concentrations for 24 h, p-JNK, JNK and p-p38 expression levels were detected by immunoblot assay. **c** HT-29 cells were transfected with TGR5 siRNA for 48 h and then treated with or without TNF-α in the presence or absence of OM8 for 24 h, p-JNK and JNK expression levels were detected by immunoblot assay. **d** ELISA analysis of cAMP levels in HT-29 cells followed by OM8 treatment for 1 h. HT-29 cells were treated with or without TNF-α in the presence or absence of OM8 for 24 h, supplemented with 3 μM MDL-12330-A (**e**) or 5 μM H89 (**f**), cleaved caspase-3, p-JNK and JNK expression were detected by immunoblot assay. Data are presented as mean ± SD ($n = 3$–5). $^{*}P < 0.05$; $^{**}P < 0.01$.

was significantly alleviated by OM8 treatment, suggesting that OM8 promoted ISC differentiation and preserved the specification of mature IECs in experimental colitis mice. Beyond the effect on ISC proliferation and differentiation, OM8 treatment significantly reduced the increased TUNEL-positive cells number in colonic epithelium and decreased the enhanced expression of cleaved caspase-3 protein in colon, suggested that OM8 might inhibit IEC apoptosis and further lead to improvement of intestinal epithelial barrier function and amelioration of colitis.

TNF-α is a common pathological factor that responsible for IEC apoptosis in colitis [7, 36]. Herein, the direct inhibition by OM8 on IEC apoptosis was further investigated in HT-29 and Caco-2 cells. OM8 toned down TNF-α induced apoptosis in HT-29 and Caco-2 cells. Meanwhile, OM8 alleviated the decreased TEER value and increased FITC-dextran flux caused by TNF-α in Caco-2 cells monolayer, suggesting that OM8 inhibited TNF-α induced IEC apoptosis and restored intestinal epithelial barrier function. Furthermore, knockdown of TGR5 by siRNA in HT-29 cells blocked the suppression of TNF-α induced apoptosis and disruption of ZO-1 protein expression and distribution induced by OM8, suggesting that OM8 inhibited TNF-α induced IEC apoptosis in a TGR5-dependent manner. Thus, our study showed the first evidence that activation of TGR5 could directly inhibit IEC apoptosis, thereby maintain intestinal epithelial barrier function and contribute to the mitigation of DSS-induced colitis.

The exact mechanism by which TGR5 activation inhibited IEC apoptosis was studied. Previous evidence suggested that JNK activation plays a crucial role in promoting TNF-α induced cell apoptosis [22–25]. Inhibition of JNK phosphorylation could reduce epithelial cell apoptosis in colitis mice [42, 43]. Besides, p38 MAPK signaling might also engage in cell apoptosis stimulated by TNF-α [24, 25]. It is also known that cAMP could inhibit the activation of JNK, thereby suppressed apoptosis [44, 45]. As a $G\alpha_s$ protein, TGR5 activation has been recognized to initiate subsequent cAMP/PKA signaling pathway [46]. Here, OM8 suppressed JNK phosphorylation and showed no obvious effect on p38 phosphorylation in HT-29 cells upon TNF-α stimulation. The inhibition by OM8 on TNF-α induced JNK phosphorylation could be obstructed upon knockdown of TGR5, indicating that OM8 inhibited TNF-α induced JNK phosphorylation in a TGR5-dependent manner. Meanwhile, AC

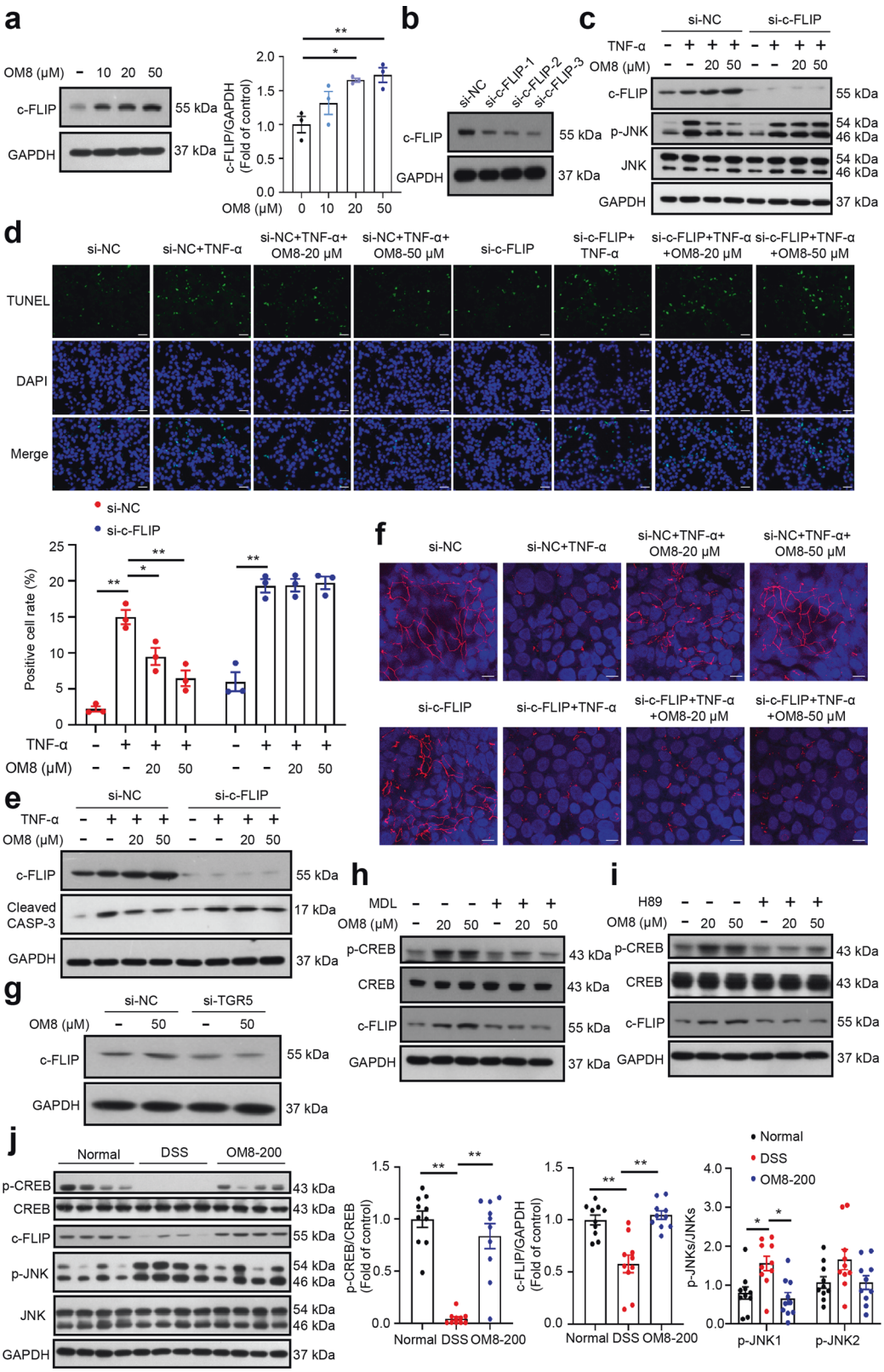

inhibitor MDL-12330-A or PKA inhibitor H89 could also completely block the suppression of TNF-α induced JNK phosphorylation and apoptosis induced by OM8 in HT-29 cells, demonstrating that TGR5 activation suppressed JNK phosphorylation by cAMP/PKA signaling pathway, thereby inhibited IEC apoptosis.

Cellular FLICE-inhibitory protein (c-FLIP), a master anti-apoptotic regulator, has been reported to inhibit apoptosis by suppressing JNK activation in certain types of cells [44, 47, 48]. Zhang et al. found that cAMP pathway could mediate c-FLIP protein expression in fibroblasts in a CREB-mediated manner [44].

Fig. 8 Upregulation of c-FLIP expression by TGR5/cAMP/PKA signaling pathway is indispensable for the inhibition by OM8 on TNF-α induced JNK phosphorylation and apoptosis in intestinal epithelial cells. **a** HT-29 cells were treated with OM8 with the indicated concentrations for 1 h, c-FLIP expression was detected by immunoblot assay. **b** The efficiency of three pairs of c-FLIP siRNA in HT-29 cells was determined by immunoblot assay. HT-29 cells were transfected with c-FLIP siRNA for 48 h and then treated with or without TNF-α in the presence or absence of OM8 for 24 h. **c** c-FLIP, p-JNK and JNK expression levels were determined by immunoblot assay. **d** Apoptotic cells were analyzed by TUNEL staining, Bar = 50 μm. **e** c-FLIP and cleaved caspase-3 expression was determined by immunoblot assay. **f** Confocal microscopy visualization of ZO-1 (red) and DAPI (blue), Bar = 10 μm. **g** HT-29 cells were transfected with TGR5 siRNA for 48 h and then treated with OM8 for 1 h, c-FLIP expression was determined by immunoblot assay. HT-29 cells were treated with OM8 in the presence or absence of 3 μM MDL-12330-A (**h**) or 5 μM H89 (**i**) for 1 h, p-CREB, CREB and c-FLIP expression levels were detected by immunoblot assay. **j** The protein levels of p-CREB, CREB, c-FLIP, p-JNK and JNK in colon. Data are presented as mean ± SD (**a**–**i**: $n = 3$–5; **j**: $n = 10$). $^{*}P < 0.05$; $^{**}P < 0.01$.

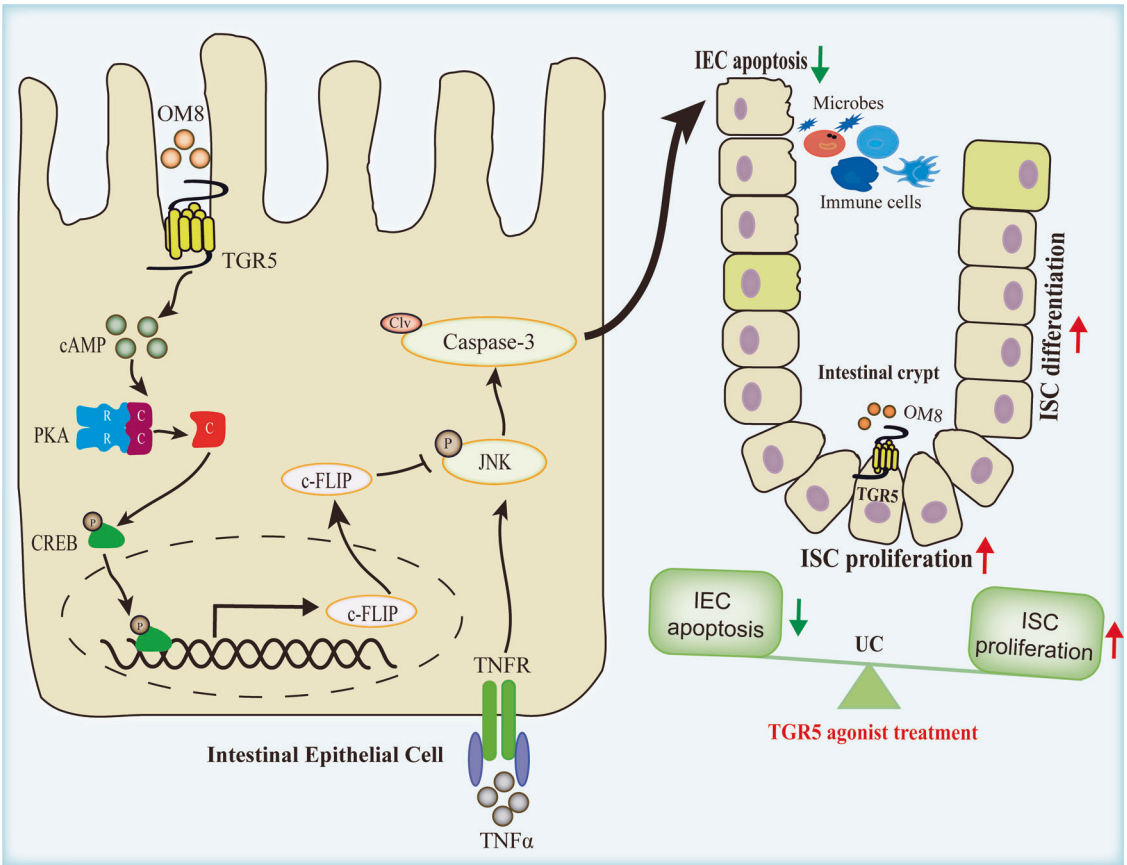

Fig. 9 Mechanisms of TGR5 agonist on inhibiting intestinal epithelial cell apoptosis and ameliorating ulcerative colitis. Activation of TGR5 by OM8 enhanced cAMP/PKA signaling, which led to upregulation of c-FLIP expression, and subsequently suppressed JNK phosphorylation, thereby antagonizing TNF-α induced intestinal epithelial cell apoptosis.

Nevertheless, the effect of TGR5 activation on c-FLIP protein expression has not been investigated and the role of c-FLIP in the pathogenesis of UC remained controversial [49, 50]. Here, OM8 upregulated c-FLIP protein expression in HT-29 cells. Knockdown of TGR5 completely abolished the upregulation of c-FLIP protein expression induced by OM8, suggesting that OM8 increased c-FLIP protein expression in a TGR5-dependent manner. Moreover, similar results were observed in treatment with MDL-12330-A or H89, indicating that TGR5 activation upregulated c-FLIP protein expression via cAMP/PKA signaling pathway. Silencing c-FLIP reversed the inhibition by OM8 on TNF-α induced JNK phosphorylation and apoptosis in HT-29 cells, implying that upregulation of c-FLIP protein expression by TGR5/cAMP/PKA axis was indispensable for the suppression of TNF-α induced JNK phosphorylation and apoptosis by OM8 in IEC. Consistently, in DSS-induced colitis mice, OM8 treatment significantly stimulated CREB phosphorylation, increased the impaired expression of c-FLIP protein and suppressed JNK phosphorylation in colon of colitis mice. These data suggested that TGR5 activation upregulated c-FLIP protein expression through cAMP/PKA signaling pathway, further suppressed JNK phosphorylation, and thereby inhibited apoptosis in IEC in vitro.

CONCLUSION

In conclusion, the present study reported a novel potent and selective TGR5 agonist OM8 with high distribution in intestinal tract, and demonstrated the beneficial effects of TGR5 activation for the treatment of DSS-induced colitis. More importantly, our study discovered that OM8 could directly inhibit TNF-α induced IEC apoptosis in a TGR5-dependent manner and identified a new mechanism that TGR5 activation inhibited IEC apoptosis via cAMP/PKA/c-FLIP/JNK signaling pathway (Fig. 9). These findings uncovered an unrecognized mechanism of TGR5 agonist on directly inhibiting IEC apoptosis in vitro, and highlighted its value as a novel therapeutic strategy for UC treatment.

ACKNOWLEDGEMENTS

This work was financially supported by National Natural Science Foundation of China (No. 81872922 and 82073683). The authors thank Dr. Wei Tang from Shanghai Institute of Materia Medica, Chinese Academy of Sciences for giving valuable suggestions.

AUTHOR CONTRIBUTIONS

YL, JHS and WJY designed the research. WJY, FHH, YPG, HQ and JL performed the research. WJY and YPG analyzed and interpreted the data. WJY and YL wrote the paper. All authors approved the final version of the manuscript.

ADDITIONAL INFORMATION

Competing interests: The authors declare no competing interests.

REFERENCES

1. Pavlidis P, Tsakmaki A, Pantazi E, Li K, Cozzetto D, Digby-Bell J, et al. Interleukin-22 regulates neutrophil recruitment in ulcerative colitis and is associated with resistance to ustekinumab therapy. Nat Commun. 2022;13:5820.
2. Gao C, Zhou Y, Chen Z, Li H, Xiao Y, Hao W, et al. Turmeric-derived nanovesicles as novel nanobiologics for targeted therapy of ulcerative colitis. Theranostics. 2022;12:5596–614.
3. Zhao J, Lin Z, Ying P, Zhao Z, Yang H, Qian J, et al. circSMAD4 promotes experimental colitis and impairs intestinal barrier functions by targeting JAK2 through sponging miR-135a-5p. J Crohns Colitis. 2022;jjac154. https://doi.org/10.1093/ecco-jcc/jjac154.
4. Scalavino V, Piccinno E, Bianco G, Schena N, Armentano R, Giannelli G, et al. The increase of miR-195-5p reduces intestinal permeability in ulcerative colitis, modulating tight junctions' expression. Int J Mol Sci. 2022;23:5840.
5. Li X, Li Q, Xiong B, Chen H, Wang X, Zhang D. Discoidin domain receptor 1(DDR1) promote intestinal barrier disruption in ulcerative colitis through tight junction proteins degradation and epithelium apoptosis. Pharmacol Res. 2022;183:106368.
6. Wan Y, Yang L, Jiang S, Qian D, Duan J. Excessive apoptosis in ulcerative colitis: crosstalk between apoptosis, ROS, ER stress, and intestinal homeostasis. Inflamm Bowel Dis. 2022;28:639–48.
7. Yu TX, Kalakonda S, Liu X, Han N, Chung HK, Xiao L, et al. Long noncoding RNA uc.230/CUG-binding protein 1 axis sustains intestinal epithelial homeostasis and response to tissue injury. JCI Insight. 2022;7:e156612.
8. Shao M, Yan Y, Zhu F, Yang X, Qi Q, Yang F, et al. Artemisinin analog SM934 alleviates epithelial barrier dysfunction via inhibiting apoptosis and caspase-1-mediated pyroptosis in experimental colitis. Front Pharmacol. 2022;13:849014.
9. Duan C, Xu X, Lu X, Wang L, Lu Z. RIP3 knockdown inhibits necroptosis of human intestinal epithelial cells via TLR4/MyD88/NF-kappaB signaling and ameliorates murine colitis. BMC Gastroenterol. 2022;22:137.
10. Rusu I, Mennillo E, Bain JL, Li Z, Sun X, Ly KM, et al. Microbial signals, MyD88, and lymphotoxin drive TNF-independent intestinal epithelial tissue damage. J Clin Invest. 2022;132:e154993.
11. Zheng C, Lu T, Fan Z. miR-200b-3p alleviates TNF-alpha-induced apoptosis and inflammation of intestinal epithelial cells and ulcerative colitis progression in rats via negatively regulating KHDRBS1. Cytotechnology. 2021;73:727–43.
12. Kawamata Y, Fujii R, Hosoya M, Harada M, Yoshida H, Miwa M, et al. A G protein-coupled receptor responsive to bile acids. J Biol Chem. 2003;278:9435–40.
13. Finn PD, Rodriguez D, Kohler J, Jiang Z, Wan S, Blanco E, et al. Intestinal TGR5 agonism improves hepatic steatosis and insulin sensitivity in Western diet-fed mice. Am J Physiol Gastrointest Liver Physiol. 2019;316:G412–G424.
14. Ma SY, Ning MM, Zou QA, Feng Y, Ye YL, Shen JH, et al. OL3, a novel low-absorbed TGR5 agonist with reduced side effects, lowered blood glucose via dual actions on TGR5 activation and DPP-4 inhibition. Acta Pharmacol Sin. 2016;37:1359–69.
15. Cipriani S, Mencarelli A, Chini MG, Distrutti E, Renga B, Bifulco G, et al. The bile acid receptor GPBAR-1 (TGR5) modulates integrity of intestinal barrier and immune response to experimental colitis. PLoS One. 2011;6:e25637.
16. Sorrentino G, Perino A, Yildiz E, El Alam G, Bou Sleiman M, Gioiello A, et al. Bile acids signal via TGR5 to activate intestinal stem cells and epithelial regeneration. Gastroenterology. 2020;159:956–68.
17. Cao H, Chen ZX, Wang K, Ning MM, Zou QA, Feng Y, et al. Intestinally-targeted TGR5 agonists equipped with quaternary ammonium have an improved hypoglycemic effect and reduced gallbladder filling effect. Sci Rep. 2016;6:28676.
18. Han F, Ning M, Wang K, Gu Y, Qu H, Leng Y, et al. Design and exploration of gut-restricted bifunctional molecule with TGR5 agonistic and DPP4 inhibitory effects for treating ulcerative colitis. Eur J Med Chem. 2022;242:114697.
19. Tang X, Ning M, Ye Y, Gu Y, Yan H, Leng Y, et al. Discovery of novel ketoxime ether derivatives with potent FXR agonistic activity, oral effectiveness and high liver/blood ratio. Bioorg Med Chem. 2021;43:116280.
20. Zou Y, Lin J, Li W, Wu Z, He Z, Huang G, et al. Huangqin-tang ameliorates dextran sodium sulphate-induced colitis by regulating intestinal epithelial cell homeostasis, inflammation and immune response. Sci Rep. 2016;6:39299.
21. Ning MM, Yang WJ, Guan WB, Gu YP, Feng Y, Leng Y. Dipeptidyl peptidase 4 inhibitor sitagliptin protected against dextran sulfate sodium-induced experimental colitis by potentiating the action of GLP-2. Acta Pharmacol Sin. 2020;41:1446–56.
22. Varfolomeev EE, Ashkenazi A. Tumor necrosis factor: an apoptosis JuNKie? Cell. 2004;116:491–7.
23. Guicciardi ME, Gores GJ. AIP1: a new player in TNF signaling. J Clin Invest. 2003;111:1813–5.
24. Jin S, Ray RM, Johnson LR. Rac1 mediates intestinal epithelial cell apoptosis via JNK. Am J Physiol Gastrointest Liver Physiol. 2006;291:G1137–1147.
25. Ibraheem K, Yhmed AMA, Nasef MM, Georgopoulos NT. TRAF3/p38-JNK signalling crosstalk with intracellular-TRAIL/Caspase-10-Induced apoptosis accelerates ROS-Driven cancer cell-specific death by CD40. Cells. 2022;11:3274.
26. Siggers RH, Hackam DJ. The role of innate immune-stimulated epithelial apoptosis during gastrointestinal inflammatory diseases. Cell Mol Life Sci. 2011;68:3623–34.
27. Mennillo E, Yang X, Paszek M, Auwerx J, Benner C, Chen S. NCoR1 protects mice from dextran sodium sulfate-induced colitis by guarding colonic crypt cells from luminal insult. Cell Mol Gastroenterol Hepatol. 2020;10:133–47.
28. Wang K, Ding Y, Xu C, Hao M, Li H, Ding L. Cldn-7 deficiency promotes experimental colitis and associated carcinogenesis by regulating intestinal epithelial integrity. Oncoimmunology. 2021;10:1923910.
29. Peterson LW, Artis D. Intestinal epithelial cells: regulators of barrier function and immune homeostasis. Nat Rev Immunol. 2014;14:141–53.
30. Lin S, Stoll B, Robinson J, Pastor JJ, Marini JC, Ipharraguerre IR, et al. Differential action of TGR5 agonists on GLP-2 secretion and promotion of intestinal adaptation in a piglet short bowel model. Am J Physiol Gastrointest Liver Physiol. 2019;316:G641–G652.
31. Watanabe S, Chen Z, Fujita K, Nishikawa M, Ueda H, Iguchi Y, et al. Hyodeoxycholic acid (HDCA) prevents development of dextran sulfate sodium (DSS)-induced colitis in mice: possible role of synergism between DSS and HDCA in increasing fecal bile acid levels. Biol Pharm Bull. 2022;45:1503–9.
32. Chen Y, Le TH, Du Q, Zhao Z, Liu Y, Zou J, et al. Genistein protects against DSS-induced colitis by inhibiting NLRP3 inflammasome via TGR5-cAMP signaling. Int Immunopharmacol. 2019;71:144–54.
33. Sakanaka T, Inoue T, Yorifuji N, Iguchi M, Fujiwara K, Narabayashi K, et al. The effects of a TGR5 agonist and a dipeptidyl peptidase IV inhibitor on dextran sulfate sodium-induced colitis in mice. J Gastroenterol Hepatol. 2015;30:60–65.
34. Gu M, Zhao P, Zhang S, Fan S, Yang L, Tong Q, et al. Betulinic acid alleviates endoplasmic reticulum stress-mediated nonalcoholic fatty liver disease through activation of farnesoid X receptors in mice. Br J Pharmacol. 2019;176:847–63.
35. Ye Z, Zhu Y, Tang N, Zhao X, Jiang J, Ma J, et al. Alpha7 nicotinic acetylcholine receptor agonist GTS-21 attenuates DSS-induced intestinal colitis by improving intestinal mucosal barrier function. Mol Med. 2022;28:59.
36. Lin W, Ma C, Su F, Jiang Y, Lai R, Zhang T, et al. Raf kinase inhibitor protein mediates intestinal epithelial cell apoptosis and promotes IBDs in humans and mice. Gut. 2017;66:597–610.
37. Xu S, Hu G, Wu D, Kan X, Oishi H, Takahashi S, et al. MafK accelerates Salmonella mucosal infection through caspase-3 activation. Aging. 2022;14:2287–303.
38. Zuo G, Zhang T, Huang L, Araujo C, Peng J, Travis Z, et al. Activation of TGR5 with INT-777 attenuates oxidative stress and neuronal apoptosis via cAMP/PKCepsilon/ALDH2 pathway after subarachnoid hemorrhage in rats. Free Radic Biol Med. 2019;143:441–53.
39. Reich M, Deutschmann K, Sommerfeld A, Klindt C, Kluge S, Kubitz R, et al. TGR5 is essential for bile acid-dependent cholangiocyte proliferation in vivo and in vitro. Gut. 2016;65:487–501.
40. Ye X, Wu J, Li J, Wang H. Anterior gradient protein 2 promotes mucosal repair in pediatric ulcerative colitis. Biomed Res Int. 2021;2021:6483860.
41. Hsu NY, Nayar S, Gettler K, Talware S, Giri M, Alter I, et al. NOX1 is essential for TNFalpha-induced intestinal epithelial ROS secretion and inhibits M cell signatures. Gut. 2023;72:654–62.
42. Assi K, Pillai R, Gomez-Munoz A, Owen D, Salh B. The specific JNK inhibitor SP600125 targets tumour necrosis factor-alpha production and epithelial cell apoptosis in acute murine colitis. Immunology. 2006;118:112–21.
43. Wang X, Cui X, Zhu C, Li M, Zhao J, Shen Z, et al. FKBP11 protects intestinal epithelial cells against inflammation-induced apoptosis via the JNK-caspase pathway in Crohn's disease. Mol Med Rep. 2018;18:4428–38.
44. Zhang J, Wang Q, Zhu N, Yu M, Shen B, Xiang J, et al. Cyclic AMP inhibits JNK activation by CREB-mediated induction of c-FLIP(L) and MKP-1, thereby antagonizing UV-induced apoptosis. Cell Death Differ. 2008;15:1654–62.

45. Zhang Y, Chen P, Liang XF, Han J, Wu XF, Yang YH, et al. Metabolic disorder induces fatty liver in Japanese seabass, Lateolabrax japonicas fed a full plant protein diet and regulated by cAMP-JNK/NF-kB-caspase signal pathway. Fish Shellfish Immunol. 2019;90:223–34.
46. Huang S, Ma S, Ning M, Yang W, Ye Y, Zhang L, et al. TGR5 agonist ameliorates insulin resistance in the skeletal muscles and improves glucose homeostasis in diabetic mice. Metabolism. 2019;99:45–56.
47. Tian F, Hu Y, Sun X, Lu G, Li Y, Yang J, et al. Suppression of cFLIPL promotes JNK activation in malignant melanoma cells. Mol Med Rep. 2016;13:2904–8.
48. Nakajima A, Kojima Y, Nakayama M, Yagita H, Okumura K, Nakano H. Down-regulation of c-FLIP promotes caspase-dependent JNK activation and reactive oxygen species accumulation in tumor cells. Oncogene. 2008;27:76–84.
49. Piao X, Komazawa-Sakon S, Nishina T, Koike M, Piao JH, Ehlken H, et al. c-FLIP maintains tissue homeostasis by preventing apoptosis and programmed necrosis. Sci Signal. 2012;5:ra93.
50. Seidelin JB, Coskun M, Vainer B, Riis L, Soendergaard C, Nielsen OH. ERK controls epithelial cell death receptor signalling and cellular FLICE-like inhibitory protein (c-FLIP) in ulcerative colitis. J Mol Med. 2013;91:839–49.